Static and dynamic back-corona characteristics

Gianluca Bacchiega, Ivo Gallimberti,
IRS srl - via Vigonovese 81 - 35124 Padova - Italy (e-mail: bacchiega@irsweb.it)

Véronique Arrondel, Philippe Raizer, Jérôme Lecointre, Michel Hamlil
EDF R&D – 6, quai Watier – 78 401 Chatou - FRANCE (e-mail : veronique.arrondel@edf.fr)

Abstract

Voltage-current characteristics are a basic tool to analyse the operational conditions of an electrostatic precipitator, and to detect the onset of Back-corona, that strongly affects the collection performances. In this investigation, a laboratory set-up has been arranged, with a classical ESP wire-plate configuration; both static and dynamic voltage-current characteristics have been measured and analysed with different geometries, dust characteristics, and layer thickness. Similar results have been also obtained in an industrial ESP, and compared with the laboratory results.

In the laboratory ESP, the static voltage-current characteristics and the collection efficiency have been measured as functions of time; with high resistivity dust, back-corona takes place as layer thickness increase, with a decrease of the efficiency and a sharp raise of the current. The effect of electrode type and powder resistivity has been analysed.
With varying applied voltages, the dynamic voltage-current characteristics show an hysteresis cycle, the recorded values depending on the slope of the applied waveform. The shape of the dynamic characteristics changes significantly with the onset of back-corona.

A self-consistent numerical model has been applied to simulate static and dynamic voltage-current characteristics in absence of back-corona. These simulations allowed to analyse the retarding effects of the different physical process (capacitive charging, ion drift, space charge movements), and to estimate the corresponding time constants. Finally, the dynamic effects of back-corona have been analysed.

A second set of experiments have been realized in a 600MW power plant: ESP static and dynamic characteristics have been measured with fly ash of low and high resistivity: the results are very similar to those obtained in the laboratory ESP, and confirm that it is possible to define a specific “signature”, on both static and dynamic V-I characteristics, of the different physical processes associated to the particle captation, including back-corona.

1 Introduction

The collection efficiency of an Electrostatic Precipitator depends on a large number of geometrical and physical parameters; the most important of them is the current emitted from the High Voltage electrodes and collected by the plates [1]: for that reason the Voltage-Current characteristic, and the actual working point on them, are used generally used to define the ESP operating conditions [2]. It is well known that in general the higher is the current the better are the collection performances. However, with high resistivity fly ash, backcorona discharges may form in the layer of deposited dust, leading to a current increase, with a reduction of the collection performances.

Backcorona is a series of micro-discharges in the air spaces within the collected dust layer [3]: it forms when an excessive field is induced in the layer by the charge flowing through its surface: it is therefore related to the local values of the current density. Backcorona forms at spots on the surface of the collecting plates, causing re-entrainment of previously collected dust. The current rises after back corona onset, and tends to be tunnelled through existing back corona spots: this accelerates the back corona growth.

Positive ions, injected by back corona into the volume of a negatively energised precipitator, have the following effects [4]:

- discharge previously charged dust particles;
- attach a positive charge to dust particles, causing their drift backwards to the emitting electrodes;
- reduce the space charge, and therefore increase the electrical field on the emitting electrode and the corona current;
- build-up nodule shaped dust deposits on the emitting electrode, that further increase local field and corona current;
- form sparks at a much lower voltage level.

In the operation of an industrial ESP it is necessary to avoid all these negative effects of backcorona: for this good diagnostic tools are needed, based on the modifications that backcorona induces on easily measurable parameters.

2 Voltage-current characteristics in a laboratory ESP model

2.1 Laboratory ESP description

The experimental tests have been performed in the Test Laboratory of SAMES in Grenoble (France) on a small scale vertical precipitator (Figure 1), made of a rectangular transparent PVC tube (0.30 x 0.30 m), with three fields, each realized with a couple of plates (Pl.1,Pl.2 and Pl.3), and two emitting electrodes. In order to test the effect of the geometry, cylindrical wires five millimetres in diameter and ribbon bands with points have been used as emitting electrodes. The applied voltage was generated by three DC switching power supplies (60kV, 500 μA), with low ripple (less than 1% peak to peak), controlled by a remote PC: this enabled to program different voltage waveshapes on each field (ramp, square, etc.).

During test operation a constant air flow of 270 m^3/h, at room temperature, was supplied to the ESP. Different types of dust were fed at the top of the precipitator duct : synthetic powders (époxy polyester, with different metal additives to vary the resistivity) and coal fly ash collected in the hoppers of an industrial ESP. The size distribution of the synthetic particles was concentrated below 10 um, while that of the coal fly ash was between 1 and 100 um. The particle resistivity could vary from medium to very high values (10^{10} to 10^{12} ohm cm). An almost constant particle concentration (10 gr/m^3) was maintained at the ESP inlet during all the test period.

Voltage and current measurements were performed at each generator, with a fast recording oscilloscope and a datalogger; the air and powder flow rates were systematically checked, to establish the inlet concentrations; the collecting plates were periodically removed and weighted (at specified time intervals 15, 30, 60 min, 1, 2, 4, 6 hr), to establish the deposition rate and the collection efficiency of each field.

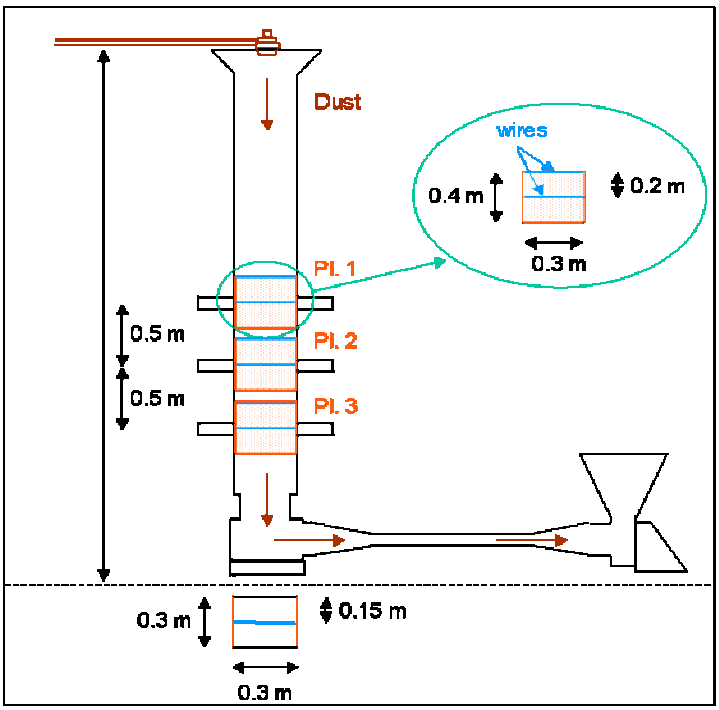

Figure 1 : Laboratory precipitator layout

2.2 Current characteristics

The corona current, under negative DC voltage, has specific patterns [5,6]]: at onset level low amplitude pulses appear, with a regular repetition rate (Trichel Pulses); as the voltage is increased, the frequency of the Trichel Pulses increases, while a continuous component is developed (Glow Corona); at even higher voltage a second impulse component appear (Pre-breakdown Streamers), with large amplitude and random pattern (Figure 2 b). If the statistical distribution of pulse amplitude is analysed, a typical double population is observed; in the present case (Figure 3), with dust load but no back-corona, the Trichel Pulses present a narrow distribution centred around 100 μA, while the pre-breakdown streamers present a wider distribution with a maximum around 250 μA.

When back-corona is established, the current pattern and the statistical distribution of pulse amplitude change completely (Figure 2 a): a new population appears of very small pulses centred around 50 μA, with random repetition rate, while the two previous ones disappear (Figure 3). These pulses have to be associated to the back-corona microdischarges in the dust layer deposited on the plates; due to their sharp form and random repetition rate they produce a wide H.F. electromagnetic noise, that makes difficult to obtain clean measurements.

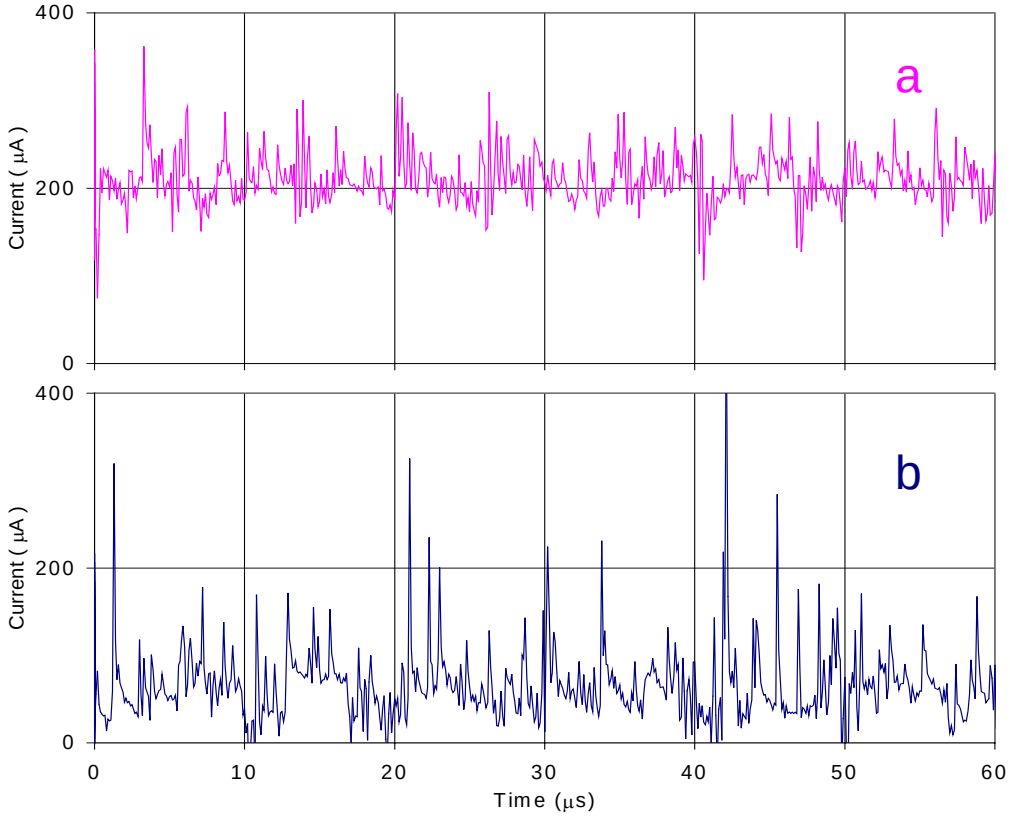

Figure 2 : current signal versus time; **b**: with dust load, V= 40 Kv, below backcorona thresold; **a** : with dust load, V= 50 Kv, above backcorona thresold

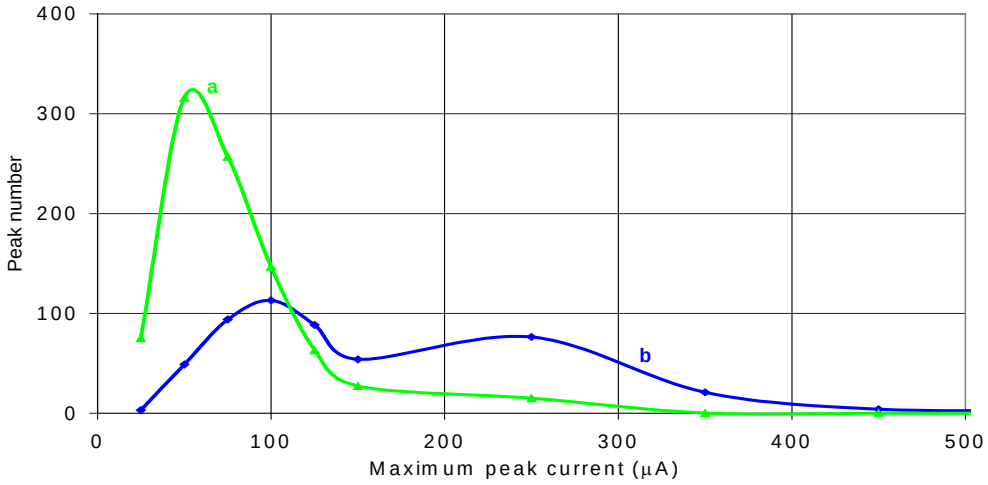

Figure 3 : Statistical distribution of current pulse amplitude; **b**: with dust load, V= 40 Kv, below backcorona thresold; **a** : with dust load, V= 50 Kv, above backcorona thresold

2.3 Static Voltage-Current characteristics

The static Voltage-Current characteristics of each field have been measured with a step by step slowly increasing voltage waveshape: with no dust load, above the corona inception threshold, all the characteristics present a typical quadratic dependence (see curve **a** in Figure 4). When a high resistivity powder is injected at top of the duct, it is possible to see that the voltage-current characteristics change in time: this variation is faster for the first plate and slower for the third one. The characteristics of Pl.3 are presented in Figure 4, after deposition times of 2, 4, 6 minutes): as the dust layer deposited on the plates increases in thickness, a back-corona discharge forms within the layer and raises the discharge current. Consequently the measured curves move to higher currents, and change shape from quadratic to linear, above the back-corona threshold.

In normal operation, the injection of low resistivity particles lowers the current values, moving the voltage-current characteristics to the right of the reference curve, with no dust load: this may be attributed to the attachment of part of the ionic charge to the particles, that have a much lower mobility; in addition, their space charge reduces the electric field on the emitting electrodes, thus reducing the corona current. On the contrary, in the present case, even in absence of back-corona, with short deposition times the characteristics is moved to the left of reference curve. This has to be attributed to an increase of the wire emissivity, associated to dust deposition on the wire surface, that increases the surface roughness and therefore the local field distortion: in this case, the field reduction due to the particle space charge is compensated by the field increase due to local distortion.

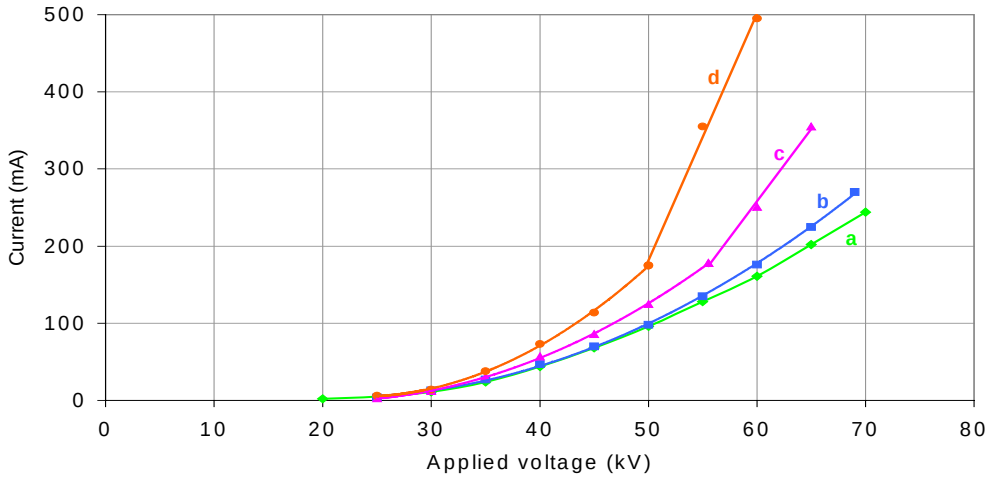

Figure 4 : Voltage-Current characteristics for different deposition times (Pl.3 - cylindrical wires; **a**=0 min; **b**=2 min; **c**=4 min; **d**=6 min)

The establishment of back-corona also affects the particle collection efficiency (see Figure 5). At the beginning of the particle injection, each plate has a slightly different efficiency (with an average around 65%), depending essentially on particle size distribution and concentration at the inlet of each plate. As the dust layer thickness increases and the back-corona forms on the plates, the particle collection efficiency decreases sharply and falls down to about 20%; the overall efficiency falls from 96% to 54%.

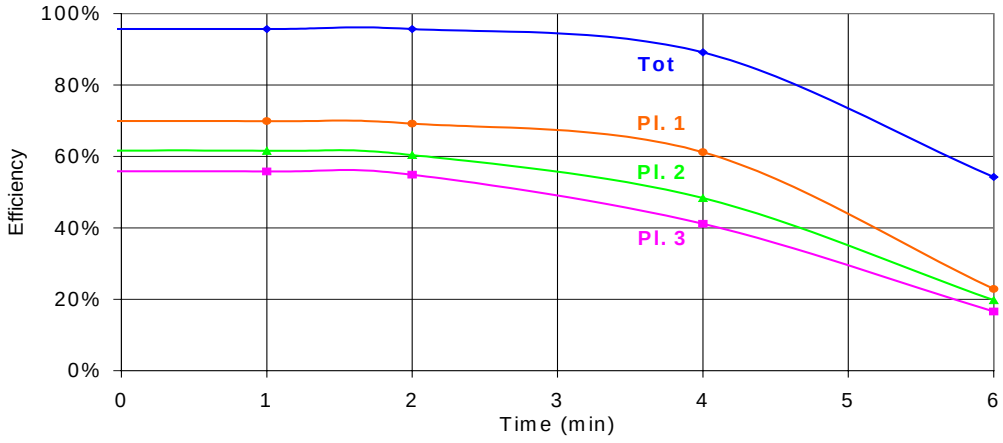

Figure 5 : Collection efficiency of the different plates as a function of deposition time (cylindrical wires, V=50 kV)

Static voltage-current characteristics with back-corona are influenced by the particle resistivity. Figure 6 show how curves change as powders with different resistivity and humidity are used. Curve **a** is given as reference without particles; curve **b** and **c** show the results for medium and high resistivity; curve **d** show the results for very high resistivity. As the resistivity increases, the field across the deposited dust layer increases, together with the back-corona intensity and the discharge current.

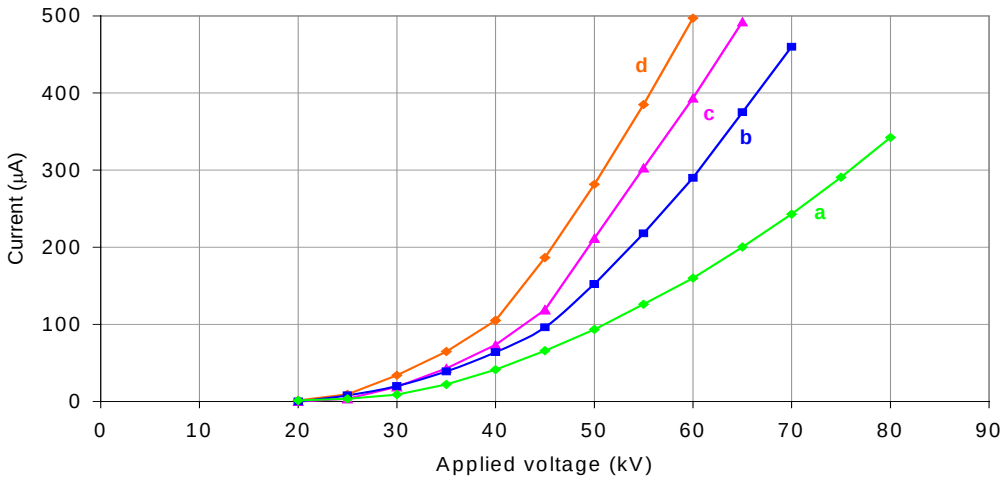

Figure 6 : Effect of particle resistivity on Voltage-current characteristics (Pl. 1 - cylindrical wires**;** **a** = no particle load; **b** = medium; **c** = high; **d** = very high)

The Voltage-current characteristics are also influenced by the geometry of the ESP electrodes. In Figure 7 the results are shown for two types of emissive electrodes: bands with points (**a**) and cylindrical wires of 5 millimetres in diameter (**b**). With no dust load, the corona voltage threshold is lower for the sharper geometry, and higher current values are obtained for lower applied voltages. A similar trend is shown by the curves with high resistivity particles (**a1** and **b1**): with the sharper geometry also the back-corona threshold becomes lower.

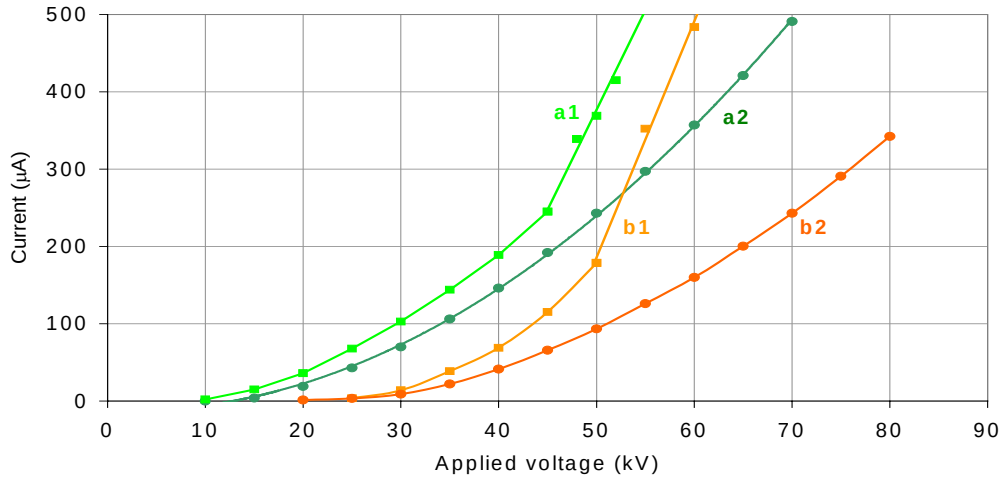

Figure 7 : Effect of the geometry of emissive electrodes on Voltage-Current characteristics (PL: 1; **a**: band with points; **b**: cylindrical wires; **1** : with dust, **2** : without dust)

It is well known from the literature [7] that the Voltage – Current characteristics has quadratic form. In the present case the form $k*U*(U - U_0)$ has been adopted, where U is the actual voltage, U_0 the corona inception voltage, and k a field distortion coefficient, that represents the effect of protrusions or points on a smooth surface: it has be assumed 1.0 for the wire, and 1.43 for the band with points. With this normalization, in absence of backcorona, the characteristics are linear, with an average slope between 0.08 and 0.10 uA/kV^2; after backcorona inception, the slope suddenly changes, and identifies with no ambiguities the inception voltage (see Figure 8). This procedure may be useful in practical applications.

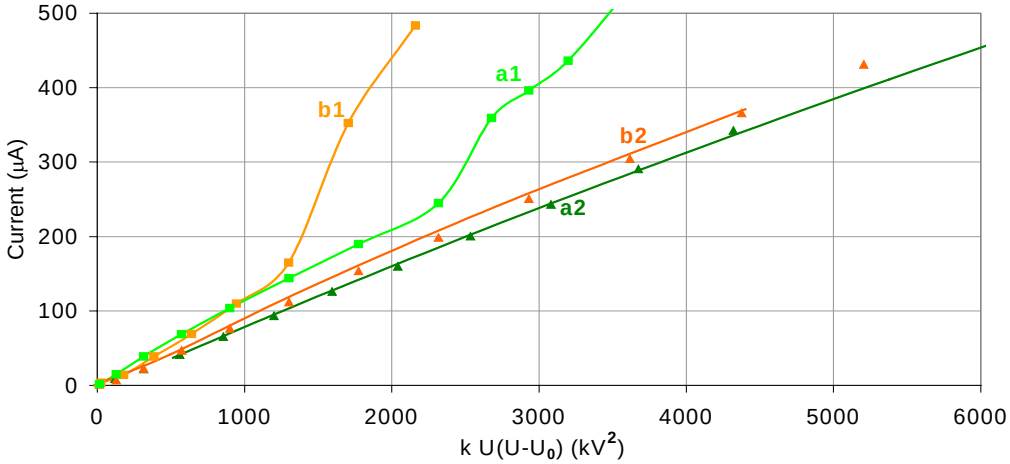

Figure 8: Curve normalization (PL: 1; **a**: band with points; **b**: cylindrical wires; **1** : with dust, **2** : without dust; **a2**, **b2** : points = experimental, lines = simulation results)

In order to verify the static characteristics on the base of the physical processes, the ORCHIDEE simulation code [8,9,10,11] has been applied to the specific conditions of the laboratory ESP. The results are reported as solid lines in Figure 8, while the points represent the experimental results: the agreement is quite satisfactory.

2.4 Dynamic voltage-current characteristics

The static Voltage-Current characteristics have been measured by applying a step by step slowly increasing voltage; if a fast varying voltage waveshape is applied, the dynamic characteristics show an hysteresis cycle, in both cases with and without dust load: an example of this behaviour is presented in Figure 9, without dust load, for bands with points as emissive electrodes, and intermittent energisation (trapezoidal wave shape with rise and fall times of the order of 30 ms). The measured current values are different depending on whether the applied voltage is increasing or decreasing: with a rising slope the current is higher than the static value, the opposite being true with a decreasing slope. This type of dynamic hysteresis cycle is typical of processes with a delayed response, which may characterized by a Time Constant: the amplitude of the hysteresis cycle depends on the steepness of the applied variation, specifically on the ratio between the Time Constant and the rise or fall times.

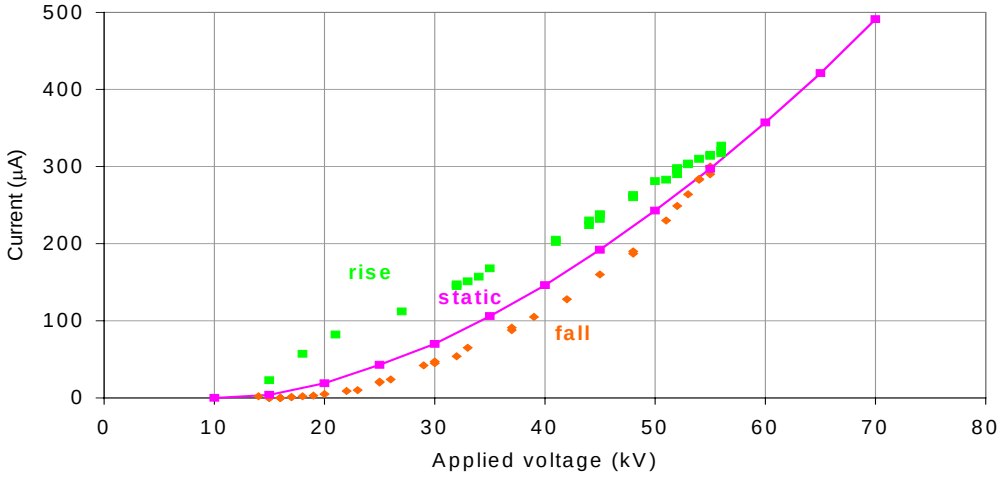

Figure 9 : Voltage-Current characteristics: static and dynamic (PL. 1; bands with points; no dust load)

In the present case, without dust load, the current is carried by the negative ions generated in the corona discharge: with a transient voltage, due to the finite mobility, their distribution between wires and plates may respond to the voltage variation only with the delay of their transport processes. Therefore, all the physical parameters associated to the current emission (space charge, electric field on the wire surface, intensity of the corona discharge) respond to voltage transient with the Time Constant of the ion transport.

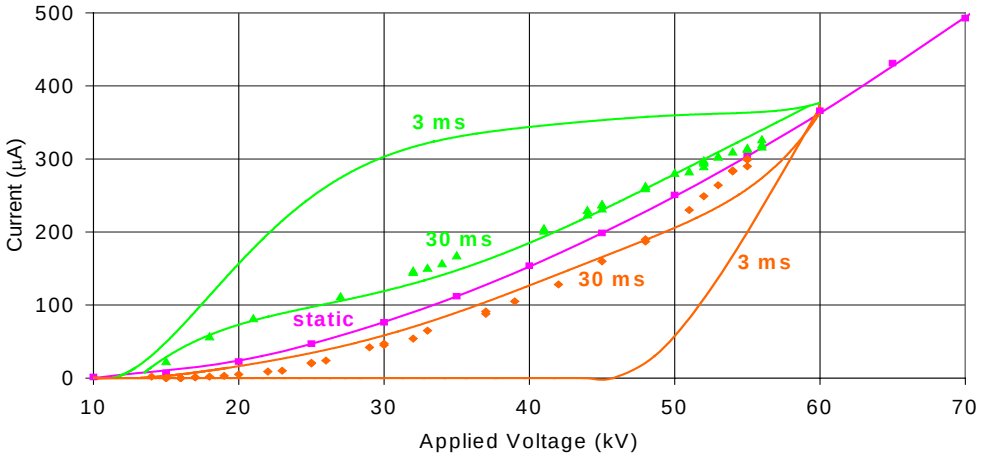

Figure 10 : Experimental (points) and simulated (lines) static and dynamic Voltage-Current characteristics (rise-fall time for simulations: 3 and 30 ms)

In order to describe in detail the dynamics of the physical processes, the ORCHIDEE simulation code [11,12] has been applied to the specific conditions of the laboratory ESP: a trapezoidal voltage waveshape has been applied, with different rise and fall times, with no dust load. The simulation results are presented in Figure 10; the lines represent the computed data, the points the experimental results. It can be clearly seen that the amplitude of the hysteresis cycle depends very much on the voltage variation rate; for a rise and fall time of 30 ms, the experimental and computed results are in quite good agreement.

The computed results show that, on the rising side of the dynamic characteristics, the voltage is in advance with respect to the space charge distribution: in fact, the charges generated around the wire need time to cross the gap and fill the volume; as a consequence of the reduced "chocking effect" of the space charge, the electric field on the wire surface is higher, leading to higher current emission. The opposite is true in the falling side: the delay in the space charge dissipation sustains the "chocking effect", and therefore reduces the field and the current.

The same behaviour is observed with the dust load, in absence of back-corona (clean plates): the amplitude of the hysteresis cycle is slightly higher, indicating a longer Time Constant for space charge transport; this is clearly due to the attachment of ions to the dust particles, and the consequent reduction of the charge average mobility. The reduced Time Constant may be assumed to result from a weighted average of the mobility Time Constants for negative ions and charged particles.

A very different behaviour is observed after the inception of back-corona (Figure 11): while the static curve steeps up rapidly, the rising side of the dynamic curve increases less rapidly than the corresponding stationary values; the dynamic values pass from the left to the right side of the static characteristics. This indicates a delay in the establishment of the back-corona discharge within the dust layer: it may be represented with a new Time Constant, which is switched on above the back-corona threshold. It is worth noting that this delay has nothing to do with that observed in par. 2.3,

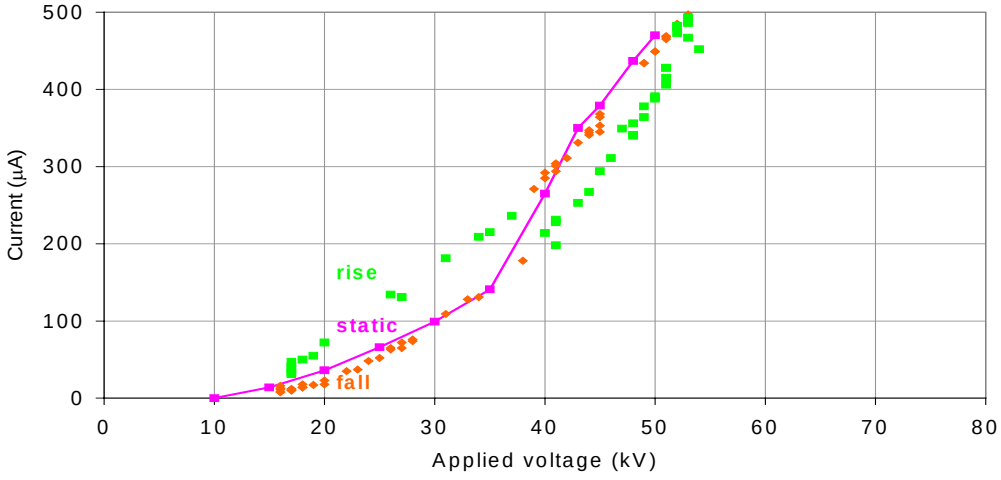

Figure 11 : Voltage-Current characteristics: static and dynamic (PL. 1; bands with points; dust load)

which was essentially associated to the rate of layer deposition on the plates. An opposite behaviour is observed in the falling part of the voltage wave (Figure 11): however, the delay for back-corona extinction appears to be quite short than that for its inception.

The shape of a 8, with the crossing of the two sides of the dynamic characteristics around the back-corona inception, seems to be a typical "signature" of the presence of back-corona discharges within the deposited dust layer: the amplitude and form the dynamic cycle may be associated to the different time constants for charge transport and discharge formation.

3 Voltage-current characteristics in an industrial ESP

3.1 Industrial ESP description

The tests on the industrial precipitator have been realized in a 600 MWe coal burning unit of the EDF Power Plant in Le Havre (France). The ESP installed at the boiler outlet is realized with three parallel casing: each of them is composed by 5 fields; the first and the last of these fields are equipped with traditional power supplies, while the other ones are equipped with new DC switching power supplies able to feed low ripple voltage (+/- 1% peak to peak). Each field has 60 gas ducts with a spacing of 0.28 m, and 7 collecting plates (0.46 m long and 12.4 m high). Emissive electrodes are 2 barbed wires per plate, placed inside rigid frames at a distance of 0.12 m each other. Rapping equipment is realized by falling hammers.

During the tests, the electrofilter flue gas flow varied from 1.25 10^6 Nm^3/h to 1.6 10^6 Nm^3/h for electrical loads varying from 410 to 530 Mwe; the fly ash concentration was roughly constant around 9 g/Nm3 (6% dry O2). Four test campaigns have been performed between March and April 2002; four different coals have been used, to test different fly ash resistivities and gas flow rates: South African coal (7 10^{10} Ohm cm – Pe = 517 Mwe), South African coal (5 10^{10} -2 10^{11} Ohm cm – Pe = 400 MW), Australian coal (3 10^9 Ohm cm – Pe = 520 MW), Polish coal (very low resistivity – Pe = 500 Mwe).

3.2 ESP static voltage-current characteristics

The industrial test have been realized in order to verify that the typical "signatures" of the backcorona formation and development, observed in the laboratory ESP model, can be effectively observed also in a full scale industrial plant.

The static Voltage-Current characteristics of each field have been measured with a step by step slowly increasing voltage. Preliminarily, a test has been realized with the plant burning high resistivity South African coal, just after the arrest of the unit. With cold precipitator (60 °C) and without dust load, two static characteristics have been recorded, before and after the evacuation of the dust layer from the plates by rapping (Figure 12). It can bee clearly seen, above 28 kV, the typical pattern of backcorona inception in the deposited dust layer.

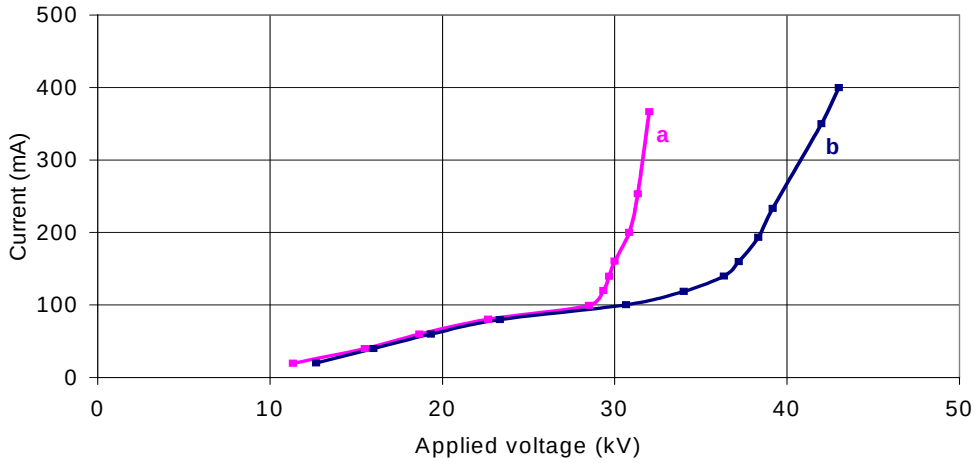

Figure 12 : Static Voltage-Current characteristics with (**a**) and without (**b**) dust layer on the plates

Similar results have been obtained under normal operating conditions: Figure 13 shows the static characteristics obtained in three different campaigns, respectively with high (**a**), medium (**b**) and low (**c**) coal resistivity.

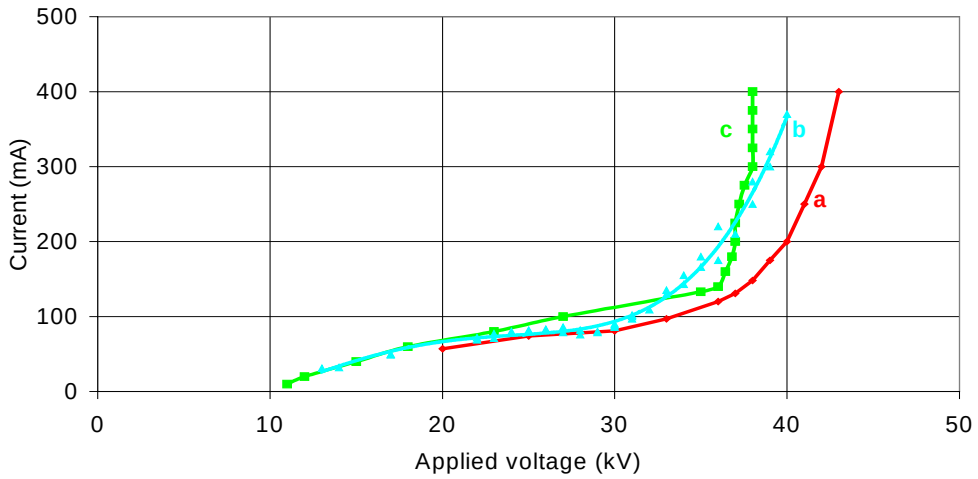

Figure 13 : Static Voltage-Current characteristics in three different campaigns, respectively with high (**a**), medium (**b**) and low (**c**) coal resistivity.

3.3 ESP dynamic voltage-current characteristics

The dynamic Voltage-Current characteristics have been recorded by applying an fast intermittent voltage waveshape: also in the industrial plant, they show an hysteresis cycle, in both cases with and without dust load: an example of this behaviour is presented in Figure 14, with dust load of low resistivity of the dust particles. As in the laboratory case, the measured current values are different depending on whether the applied voltage is increasing or decreasing: with a rising slope the current is higher than the static value, the opposite being true with a decreasing slope.

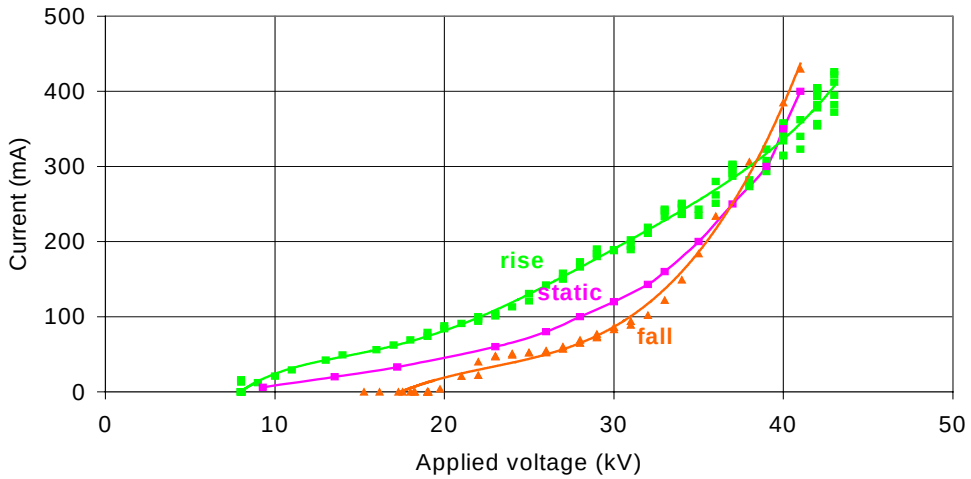

Figure 14 : Voltage-Current characteristics: static and dynamic (Polish coal, with low resistivity).

As in the laboratory case, a very different behaviour is observed with high resistivity dust (5): when the static curve steeps up rapidly, the rising side of the dynamic curve increases less rapidly passing from the left to the right side of the static characteristics; the opposite is true for the falling side of the characteristics. Also in the industrial ESP, the shape of a 8, with the crossing of the two sides of the dynamic characteristics around the back-corona inception, seems to be the typical “signature” of the presence of back-corona discharges within the deposited dust layer.

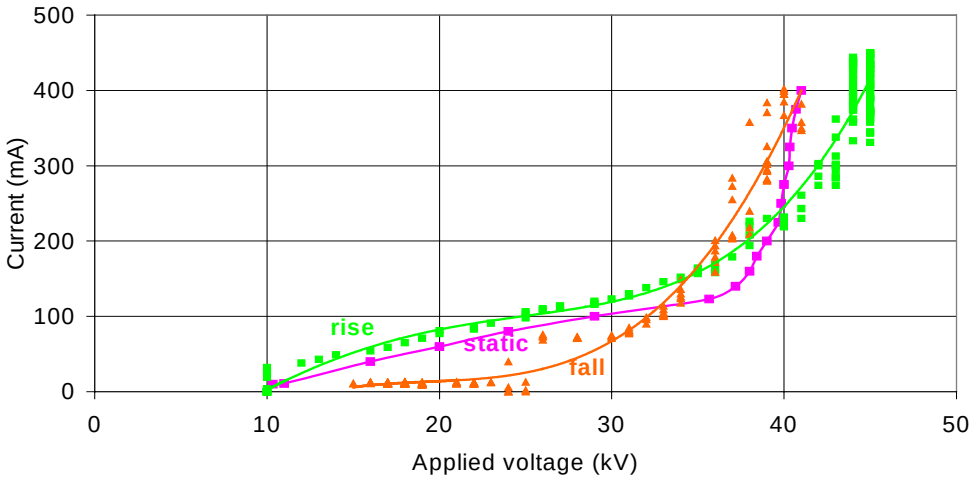

Figure 15 : Voltage-Current characteristics: static and dynamic (South African coal, with high resistivity).

Conclusions

In this paper the typical “signatures” , that identify the onset of backcorona, have been presented and discussed:

- a change in the impulse component of the discharge current, which moves the statistical distribution of the peak amplitudes towards lower values;
- a steep change of the static Voltage-Current characteristics at onset threshold, particularly evident on normalized curves;
- the appearance of a 8 shaped form in the dynamic Voltage-Current hysteresis cycle, with a crossing point around the onset conditions;

The analysis of these “signatures” may be recommended as a technique to determine the onset of back corona, and to analyse the susceptibility of a precipitator to back corona, under specific operating conditions.

Acknowledgements

The authors wish to thank the Company SAMES in Grenoble, its technical director Caryl Thomé, and its personnel, for the use of the laboratory equipment, and for the help in running the tests. The authors are also indebt with the personnel of the Le Havre power plant for the participation to the industrial ESP tests.

References

[1] S. OGLESBY, G. NICHOLS: “Electrostatic precipitation”, Dekker, New York, 1978

[2] R.J. TRUCE, W. REIBELT: "New technologies improves electrostatic precipitator performances”, VII ICESP*, Kyongjiu (Korea), 1998

[3] S. MASUDA, A. MIZUNO: “Initiation condition and mode of back-discharge”, Journal of Electrostatics 4, 1977-78

[4] R.J. TRUCE, “Back Corona and its Effects on the Optimisation of electrostatic Precipitator Energisation control”, Seventh International Clean Air Conference, August 24-28, 1981

[5] L. B. LOEB: “Electrical Coronas”, University of California Press: Berkeley, CA ,1965

[6] A. VALAGUSSA: “Prove di laboratorio per lo studio della captazione elettrostatica”, Rapp. CESI Lab-93/3138, 1995

[7] I. GALLIMBERTI : “The mechanism of the long spark formation”, J. de physique, colloque C7, supplement au n.7, Tome 40, Juillet 1979

[8] I. GALLIMBERTI, A. GAZZANI, U. TROMBONI, E. LAMI, F. MATTACHINI, G. TREBBI:"Physical simulation of the particle migration in ESP, Part I - Model description", VI ICESP*, Budapest, 1996.

[9] I. GALLIMBERTI, A. GAZZANI, U. TROMBONI, E. LAMI, F. MATTACHINI, G. TREBBI:"Physical simulation of the particle migration in ESP, Part II - Application results", VI ICESP*, Budapest, 1996.

[10] E. LAMI, F. MATTACHINI, I. GALLIMBERTI, R. TURRI, U. TROMBONI: "A Numerical Procedure for Computing the Voltage-Current Characteristics in ESP Configuration", Journal of Electrostatics 34 p.385-399, 1995.

[11] I. GALLIMBERTI: "Recent advancements in the physical modelling of electrostatic precipitators", Journal of Electrostatics 43 (1998) 219-247, 1998
.
[12] V. ARRONDEL, G. BACCHIEGA, I.GALLIMBERTI: "ESP modelling: from University to Industrial Application", VIII ICESP, Birmingham (USA), 2001